SiGe Island Shape Transitions Induced by Elastic Repulsion

J. A. Floro,[1] G. A. Lucadamo,[2] E. Chason,[1] L. B. Freund,[3] M. Sinclair,[1] R. D. Twesten,[4] and R. Q. Hwang[5]
[1]*Sandia National Laboratories, Albuquerque, New Mexico 87185-1415*
[2]*Lehigh University, Department of Materials Science and Engineering, Bethlehem, Pennsylvania 18015-3915*
[3]*Division of Engineering, Brown University, Providence, Rhode Island 02912*
[4]*University of Illinois, Center for Microanalysis of Materials, Urbana, Illinois 61801*
[5]*Sandia National Laboratories, Livermore, California 94551*
(Received 7 January 1998; revised manuscript received 20 March 1998)

The detailed morphological evolution during the transition between hut clusters and dome clusters is examined for $Si_{0.8}Ge_{0.2}/Si(001)$ heteroepitaxy. Simultaneous real-time light scattering and stress measurements directly demonstrate the correlation between island impingement and the shape transformation. We show that elastic interactions between islands can significantly reduce the equilibrium transition volume and may also modify the activation barrier for the transition. [S0031-9007(98)06223-1]

PACS numbers: 68.35.Bs, 68.55.–a, 81.15.–z

Coherent island formation provides a pathway to strain relaxation during lattice-mismatched heteroepitaxy that can bypass, or at least precede, dislocation introduction [1–6]. Relaxation results from the evolution of the film geometry rather than through shear, and is kinetically mediated by surface diffusion. Strain not only drives the initial 2D-to-3D transition during growth, but can also drive transitions from one island shape to another [6–12]. Island shape transitions are of interest because they probe the energetics and kinetic pathways associated with deterministic morphological evolution arising from the competition between strain energy and surface energy. These issues are critical to producing dense arrays of islands of controlled size for quantum dot applications.

In a previous publication, we showed that the sequence of island transitions during $Si_{0.8}Ge_{0.2}/Si(001)$ heteroepitaxy (0.8% lattice mismatch strain) mirrors that observed for Ge/Si(001) heteroepitaxy (4% strain), as long as the growth temperature is high enough to provide sufficient adatom mobility [11]. Longer surface diffusion lengths are required to overcome kinetic limitations imposed by the low strain. In particular, there is a natural length scale associated with strain-driven islanding that is proportional to $\Delta\Gamma/M\varepsilon_{\rm coh}^2$, where $\Delta\Gamma$ is the change in surface energy, M is an elastic modulus, and $\varepsilon_{\rm coh}$ is the lattice mismatch strain. Length scaling in the low strain regime can be exploited in the study of islanding phenomena, since transitions are a more gradual function of film thickness, allowing easier observation of intermediate transition stages, and since the increased length scales allow use of real-time optical probes.

In this Letter, we examine the detailed transition from the hut cluster morphology (pyramidal islands bound by [501] facets [1]) to the dome cluster morphology (more isotropic island predominantly bound by [311] facets [8]) during $Si_{0.8}Ge_{0.2}/Si(001)$ heteroepitaxy. We show that island-island elastic interactions can strongly modify the transition energetics.

$Si_{0.8}Ge_{0.2}$ films were grown by molecular beam epitaxy (MBE) on Si(001) at 755 ± 10 °C and 0.1 Å/s to various thicknesses [12]. All film thicknesses quoted here are mass equivalent thicknesses. The films are imaged *ex situ* using scanning electron microscopy (SEM), atomic force microscopy (AFM), and transmission electron microscopy (TEM).

Figure 1 shows a sequence of SEM images at different film thicknesses following the evolution from a pure array of [501]-faceted huts to a pure array of domes [Fig. 1(e)]. We showed previously that, under the current growth conditions, the film exhibits a compact hut cluster morphology from 60 to almost 130 Å thickness. In this regime, the [501] facet appears extremely stable—the huts grow, but retain their essential shape [11]. At 130 Å, the areal coverage of huts approaches unity and

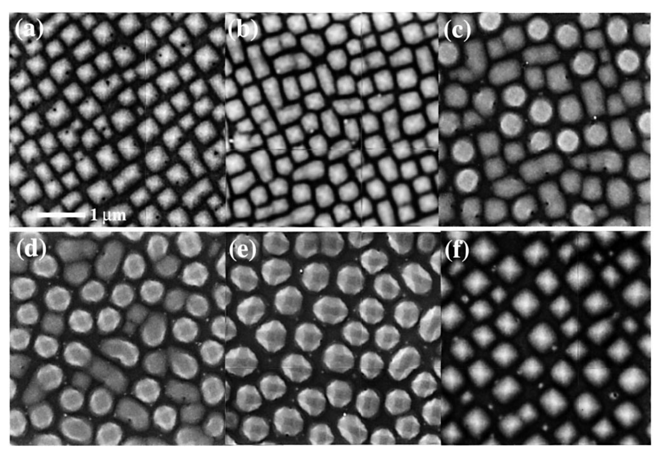

FIG. 1. SEM images showing the evolution from huts to domes as a function of $Si_{0.8}Ge_{0.2}$ equivalent thickness (six different depositions). All images are the same magnification. (a) 104, (b) 130, (c) 170, (d) 230, and (e) 275 Å. (f) SEM image of a film grown to 104 Å and then annealed to promote static coarsening. Compare hut size and spacing with that in (a).

copious impingement of neighboring huts occurs, shown in Fig. 1(b). At this point, the [501] facet destabilizes, and the island shape evolves rapidly.

In order to quantitatively demonstrate the connection between hut impingement and the transformation to domes, we have made real-time measurements during MBE growth of both the film stress, using a curvature-based technique [11,12], and the mean spatial period of the island array. The latter is accomplished using a novel optical scattering technique that employs broadband illumination of the substrate and spectroscopic detection of the backscattered light. The islands act like a diffraction grating, resulting in a peak in the optical scattering spectrum, measured along a $\langle 100\rangle$ azimuth, that can be correlated with the mean island separation [13]. Part of the motivation for developing a real-time monitor of island spacing is our observation that the spacing, size, and areal density of islands are very sensitive to the deposition temperature, making *ex situ* measurement of the *evolution* of these characteristics rather difficult.

In Fig. 2(a), we plot the stress-thickness product [14], and the mean island spacing λ, as a function of equivalent thickness h during MBE growth. The pure [501]-hut regime during deposition, which is characterized by a constant effective stress due to the constant island shape [22], is shown as the shaded region in Fig. 2. At $h \approx 130$ Å, the effective film stress begins to drop, signaling the onset of the hut-to-dome transition. The stress reduction occurs because the island facet angle steepens beyond that of [501], thereby increasing the island aspect ratio [11,15]. Plan-view TEM verifies the film to be dislocation-free throughout the transition. Within the hut regime we observe the hut spacing $\lambda(h)$ to *increase* with thickness; i.e., the areal density (number per unit area) of islands decreases, implying that the huts coarsen during growth [16]. From the $\lambda(h)$ data, we determine the mean island volume as $V = (h - h_{\mathrm{wl}})\lambda^2$, where h_{wl} is the wetting layer thickness, here taken to be 22 Å [11]. $V(h)$ is shown in Fig. 2(b), where the critical volume V_c at the hut-to-dome transition is also explicitly identified.

The fixed island shape in the hut regime allows us to quantitatively determine the areal coverage $\theta(h)$ of the hut clusters from the $\lambda(h)$ data: $\theta = [A(h - h_{\mathrm{wl}})/\lambda]^{2/3}$, where A is a dimensionless geometric factor equal to 30 to compact [501] huts. Figure 2(c) shows that $\theta(h)$ increases rapidly with film thickness [17]. The key observation is that the coverage approaches unity at the same thickness (130 Å) that the film stress begins to drop at the beginning of the hut-to-dome transition. Thus the combined stress and areal coverage data of Fig. 2 explicitly demonstrate the correlation between hut impingement and the onset of the shape transformation.

We performed annealing experiments to suppress impingement and examine the effect on the hut-to-dome transition. A $Si_{0.8}Ge_{0.2}$ film was grown to 104 Å equivalent thickness at 755 °C and then annealed at the growth temperature for 45 minutes. After the anneal, the islands

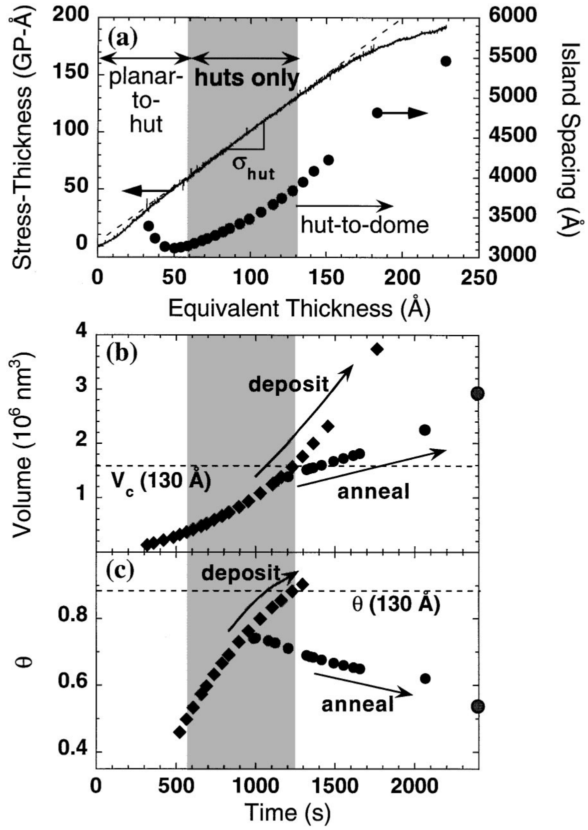

FIG. 2. (a) Stress thickness determined from real-time wafer curvature measurement during MBE growth of $Si_{0.8}Ge_{0.2}$. The slope represents the effective film stress. Also, the mean spacing of the island array determined from spectroscopic light scattering. (b) The mean island volume and (c) the areal coverage, from the light scattering data, as a function of deposition *time* (deposition rate $= 0.104$ Å/s). The diamond symbols are for continuous deposition wile the circles are for annealing. The gray circles are data from *ex situ* imaging at $t = 3700$ s.

were imaged *ex situ* by SEM [Fig. 1(f)] and AFM. We find that the island array coarsened, reducing the areal coverage to $\theta \approx 0.5$, compared with $\theta \approx 0.9$ for continuous growth to 130 Å, as shown in Fig. 2(c). Concurrently, the mean island volume coarsened to become 1.9 times larger than V_c for the 130 Å thick film, as shown in Fig. 2(b). Throughout the entire anneal, the islands retained the compact hut cluster morphology—no transformation to domes was observed. We will argue that this result does not arise from metastability due to kinetic constraints, but instead that the *energetics* of the shape transition are modified by elastic interactions between islands at high areal coverage.

Islands interact repulsively through their mutual strain fields in the substrate [15]. The presence of nearby islands makes the substrate appear stiffer, thereby reducing the overall elastic relaxation. We can incorporate the effect of elastic interactions into the overall system energetics in a simple fashion. The mean island volume is $V = h\lambda^2$, where λ is the spacing between neighboring islands, and

h is the equivalent thickness. The energy per unit area, relative to planar film of the same thickness, is given by

$$\Delta E_A = \frac{\Delta E_{\mathrm{tot}}}{\lambda^2} = M\varepsilon^2 h\{G[1 + f(\theta)] - 1\} + \Delta\Gamma h V^{-1/3}, \quad (1)$$

where M is the biaxial modulus, $\Delta\Gamma$ is the change in surface energy upon island formation, and G is the fractional reduction in average strain energy density associated with the island shape ($0 < G \leq 1$). The areal coverage of islands, θ, can be expressed as $\theta = KhV^{-1/3}$, where K depends only on island shape. The function $f(\theta)$ describes the additional elastic energy density imposed by island interactions. Figure 3(a) illustrates how elastic interactions affect the transition volume. The solid curves represent the areal energy density for zero coverage [18]. The crossing point is the critical volume V_0 for the transition of an isolated hut to a dome. The dashed curves represent the areal energy density at nonzero coverage. In general, $V_c \neq V_0$ when elastic interactions are significant.

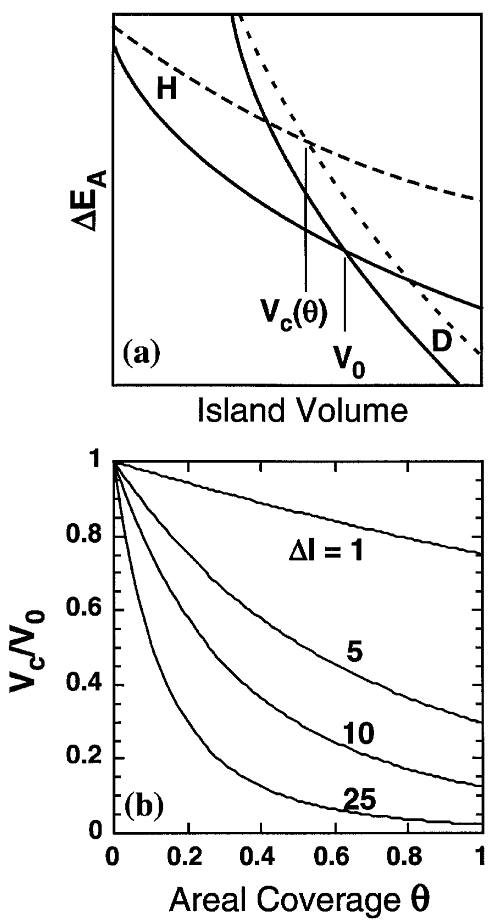

FIG. 3. (a) Schematic illustration of the areal energy density as a function of island volume at zero coverage (solid lines) and finite coverage (dashed lines) for huts (H) and domes (D). The transition volume V_0 is reduced to V_c at finite coverage. (b) The reduction in V_c as a function of coverage calculated from Eq. (2) for several values of the interaction parameter.

We performed 2D finite element calculations of the increase in elastic energy density as a function of lineal coverage of triangular islands. The results can be fit to a parametric form $f(\theta) = Q\theta^n$, which was also used in an analytical analysis by Shchukin *et al.* [19]. The equilibrium transition volume is then obtained by setting $\Delta E_{A,\mathrm{huts}}(V,\theta) = \Delta E_{A,\mathrm{domes}}(V,\theta)$, and solving for V_c [20]:

$$\frac{V_c}{V_0} = \left[1 + \Delta I\left(\frac{\theta}{K}\right)^n\right]^{-3}, \quad (2)$$

where $\Delta I = (G_H Q_H K_H^n - G_D Q_D K_D^n)/(G_H - G_D)$ and $V_0^{1/3} = (\Delta\Gamma_D - \Delta\Gamma_H)/[M\varepsilon^2(G_H - G_D)]$. The subscripts H and D refer to huts and domes, respectively. Note that the essential strain scaling is captured in V_0.

Shchukin used a value of $n = 1.5$ [19], but our finite element calculations of the elastic interaction energy are best fit by $n = 1$. In Fig. 3(b), we plot V_c/V_0 (for $n = 1$) as a function of coverage for several values of the interaction parameter ΔI. The important result is that the critical volume for the hut-to-dome transition can be strongly reduced by elastic interactions. We estimate that a value of $\Delta I \approx 20$ is quite reasonable for this transition [21]. A different value of the exponent n will affect the quantitative result, but does not change the essential conclusion that elastic interactions significantly modify the transition volume.

In the annealing experiment described earlier, we did not anneal long enough to observe the true V_0, which will be quite large at low strain. However, a recent experiment involving near-equilibrium growth of pure Ge on Si(001) was performed by Medeiros-Ribeiro *et al.* [22,23]. In this work, reversible transitions of huts into domes were observed at very low areal coverage. The transition volume ($\approx V_0$) in these experiments is about 50 times larger than that reported for Ge/Si(001) by Tomitori *et al.* [8], whose growth conditions resulted in hut impingement, followed by transitions to dome clusters. $V_c = 50V_0$ implies a value of $\Delta I = 25$ from Eq. (2), with $n = 1$. This result is consistent with our analysis, and supports the contention that our annealed hut clusters are not metastable, but in fact are still in the energetically stable regime in the absence of elastic interactions.

It must be pointed out that Medeiros-Ribeiro *et al.* also show strong evidence for a preferred island size [22,23], as was first predicted theoretically by Shchukin *et al.* [19]. In order to observe a preferred island size, the elastic contributions of the island edges must contribute significantly to the total energy. Bulk-strain-induced reduction of the effective surface energy [19,24] is also very important [22]. However, at low strain and large island size, the edges contribute negligibly to the total energy, and surface energy changes are expected to still act as a barrier to island formation and shape transitions. Thus we feel it is justified to use the simpler analysis associated with Eq. (1) to describe the transition energetics characterizing our experimental results.

In addition to reducing the critical volume for the hut-to-dome transition, elastic interactions between islands can also reduce the activation barrier associated with the transition. The barrier arises from the local increase in energy, due to surface energy anisotropy, for island shapes intermediate between huts and domes. Short-range elastic interactions create a gradient in chemical potential along the island surface. We used our 2D finite element model to evaluate the elastic energy density along the surface of the [501] facet, as a function of areal coverage. We find that, as the islands approach closer than one-tenth their length, the gradient in the elastic chemical potential at the corner rises rapidly [25]. This could effectively destabilize the [501] facet by piling up adatoms away from the corner and roughening the surface, thereby fostering nucleation of a steeper facet. The [311] facet eventually "locks in" as a local minimum in the Wulff surface.

This conceptual model is consistent with our observations of the intermediate stages of transition. Figure 1 shows that, beyond 130 Å thickness, huts elongate to form ridges that are a kinetically defined intermediate configuration. AFM profiles verify that the ridge facets are significantly steeper than [501]. By 170 Å thickness, compact domes with steep [h11] facets form via ridge fission. As the film thickens, dome formation continues, and the dome facet approaches [311]. Jesson has described a qualitatively similar sequence of transitions in $Si_{0.5}Ge_{0.5}$ during annealing [7]. When the transformation is complete the domes are fully compact, isolated, and highly faceted.

In summary, we used simultaneous real-time measurements of stress and surface spatial period to directly verify the correlation between hut cluster impingement and the onset of the hut-to-dome transition. High areal coverage is kinetically imposed by the deposition process. Static annealing experiments demonstrate that the critical volume for the transition can be made much larger when impingement is avoided. A simple energetic analysis that includes elastic interactions between islands captures the essentials of this behavior.

We thank John Hunter for his assistance with the MBE growths, Bob Cammarata for his insights, and Bonnie McKenzie for her excellent SEM work. We are grateful to Stan Williams for very useful discussions and for sharing unpublished information. L. B. F. acknowledges the MRSEC program at Brown University funded by the National Science Foundation under Award No. DMR-9632524. Sandia is a multiprogram laboratory operated by Sandia Corporation, a Lockheed Martin Company, for the United States Department of Energy under Contract No. DE-AC04-94AL85000.

[1] Y.-W. Mo, D. E. Savage, B. S. Swartzentruber, and M. G. Lagally, Phys. Rev. Lett. **65**, 1020 (1990).
[2] D. J. Eaglesham and M. Cerullo, Phys. Rev. Lett. **64**, 1943 (1990).
[3] S. Guha, A. Madhukar, and K. C. Rajkumar, Appl. Phys. Lett. **57**, 2110 (1990).
[4] D. E. Jesson, K. M. Chen, S. J. Pennycook, T. Thundat, and R. J. Warmack, Science **268**, 1161 (1995).
[5] J. Tersoff and F. K. LeGoues, Phys. Rev. Lett. **72**, 3570 (1994).
[6] M. Hammar, F. K. LeGoues, J. Tersoff, M. C. Reuter, and R. M. Tromp, Surf. Sci. **349**, 129 (1996).
[7] D. E. Jesson, K. M. Chen, S. J. Pennycook, T. Thundat, and R. J. Warmack, J. Electron. Mater. **26**, 1039 (1997).
[8] M. Tomitori, K. Watanabe, M. Kobayashi, and O. Nishikawa, Appl. Surf. Sci. **76/77**, 322 (1994).
[9] T. I. Kamins, E. C. Carr, R. S. Williams, and S. J. Rosner, J. Appl. Phys. **81**, 211 (1997).
[10] M. Goryll, L. Vescan, K. Schmidt, S. Mesters, H. Lüth, and K. Szot, Appl. Phys. Lett. **71**, 410 (1997).
[11] J. A. Floro, E. Chason, R. D. Twesten, R. Q. Hwang, and L. B. Freund, Phys. Rev. Lett. **79**, 3946 (1997).
[12] J. A. Floro, E. Chason, S. R. Lee, R. D. Twesten, R. Q. Hwang, and L. B. Freund, J. Electron. Mater. **26**, 983 (1997).
[13] E. Chason, M. Sinclair, J. A. Floro, and G. A. Lucadamo (to be published).
[14] Curvature techniques measure bending moments that are the product of the film stress and film thickness [12]. The slope of the stress-thickness curve is the effective stress. We define the effective stress as the stress in a uniform-thickness, mass-equivalent layer that produces the same curvature as the islanded layer.
[15] H. T. Johnson and L. B. Freund, J. Appl. Phys. **81**, 6081 (1997).
[16] Note that the areal density of islands in Fig. 1(b) exceeds that of Fig. 1(a). This results from the sensitivity to growth temperature mentioned in the text—in this case arising from a 15° difference in deposition temperature.
[17] We emphasize that the assumption of fixed island shape is only strictly valid in the thickness range of 60–120 Å. Outside this range $\theta(h)$ may be slightly overestimated, but the trend of increasing θ with film thickness remains relevant.
[18] F. M. Ross, J. Tersoff, and R. M. Tromp, Phys. Rev. Lett. **80**, 984 (1998).
[19] V. A. Shchukin, N. N. Ledentsov, P. S. Kop'ev, and D. Bimberg, Phys. Rev. Lett. **75**, 2968 (1995).
[20] For simplicity, we treat domes as pyramids with a steeper facet angle β. The essential results are not affected by a more rigorous treatment of the island geometry.
[21] We note that negative values of $\Delta\tilde{\Theta}$ will *increase* the critical volume. A negative value results if the elastic interaction energy between domes at a given film thickness and volume exceeds the interaction between huts.
[22] Gilberto Medeiros-Ribeiro, Alexander M. Bratkovski, Theodore I. Kamins, Douglas A. A. Ohlberg, and R. Stanley Williams *et al.*, Science **279**, 353 (1998).
[23] T. I. Kamins, G. Medeiros-Ribeiro, D. A. A. Ohlberg, and R. Stanley Williams (to be published); G. Medeiros-Ribeiro, T. I. Kamins, D. A. A. Ohlberg, and R. Stanley Williams (to be published).
[24] R. C. Cammarata, Prog. Surf. Sci. **46**, 1 (1994).
[25] J. A. Floro, E. Chason, L. B. Freund, R. D. Twesten, M. Sinclair, G. A. Lucadamo, and R. Q. Hwang (to be published).